IEEE Access
Multidisciplinary ⋮ Rapid Review ⋮ Open Access Journal

Received January 11, 2021, accepted January 27, 2021, date of publication February 1, 2021, date of current version February 10, 2021.

*Digital Object Identifier 10.1109/ACCESS.2021.3056244*

# ICEBIN: Image Contrast Enhancement Based on Induced Norm and Local Patch Approaches

**TZU-CHIA TUNG[1] AND CHIOU-SHANN FUH[2], (Member, IEEE)**
[1]Graduate Institute of Networking and Multimedia, National Taiwan University, Taipei 10617, Taiwan
[2]Department of Computer Science and Information Engineering, National Taiwan University, Taipei 10617, Taiwan

Corresponding author: Tzu-Chia Tung (d04944016@ntu.edu.tw)

This work was supported by the Ministry of Science and Technology of Taiwan, R.O.C., under Grants MOST 109-2221-E-002-158-MY2 and MOST 108-2221-E-002-140, and by Test Research, Jorgin Technologies, III, Chernger, ARCS Precision Technology, D8AI, PSL, and LVI.

**ABSTRACT** Traditional histogram equalization may cause degraded results of over-enhanced images under uneven illuminations. In this paper, a simple and effective image contrast enhancement method is proposed to achieve high dynamic range imaging. First, the illumination of each pixel is estimated by using an induced norm of a patch of the image. Second, a pre-gamma correction is proposed to enhance the contrast of the illumination component appropriately. The parameters of gamma correction are set dynamically based on the local patch of the image. Third, an automatic Contrast-Limited Adaptive Histogram Equalization (CLAHE) whose clip point is automatically set is applied to the processed image for further image contrast enhancement. Fourth, a noise reduction algorithm based on the local patch is developed to reduce image noise and increase image quality. Finally, a post-gamma correction is applied to slightly enhance the dark regions of images and not affect the brighter areas. Experimental results show that the proposed method has its superiority over several state-of-the-art enhancement quality techniques by using qualitative and quantitative evaluations.

**INDEX TERMS** Contrast enhancement, contrast-limited adaptive histogram equalization, gamma correction, high dynamic range, induced norm, noise reduction.

## I. INTRODUCTION

Recently, the requirement for digital photography and multimedia applications has been increasing. One of these requirements is to obtain as much complete image dynamic range information as possible, which is called High Dynamic Range (HDR) imaging. HDR aims to overcome the shortcomings of traditional images and display a wide exposure dynamic range. Therefore, under the environment of significant difference between light and shadow, the details of the bright and dark areas of a photograph of HDR can still be retained. HDR digital imaging uses a combination of contrast ratio and an observer-based color perception model and multiple exposures of a single scene to improve visual authenticity.

In addition to using sensors to achieve HDR, image synthesis with multiple exposures is also a feasible solution [1]–[4]. HDR has become one of the main fields of computer graphics so far [5]. Because HDR can show the appearance of real scenes, it has become more and more popular. In the photography world, HDR has attracted many professional and amateur photographers and has practicality in many applications such as visual effects production. Although some specific cameras can be used to capture HDR images directly, they are still expensive and not popular. Nowadays, mobile devices with cameras such as smartphones or tablets have become more and more popular and lead to many photographs in our daily lives. Some photos produced under the complicated factors of the lighting environment result in lower visibility. Many contrast enhancement methods have been developed to solve this problem, where the mainstream can be divided into two categories: based on histogram and based on Retinex.

The former is based on the intensity level distribution in the input image to explore the ideal dynamic range to enhance the contrast. For example, Histogram Equalization (HE) and its modifications are easily combined with several optimization techniques to adjust the intensity distribution of the original image effectively. Histogram equalization flattens the intensity histogram and extends the dynamic range of intensity levels. It is the most well-known method because of its simplicity and effectiveness. However, the recovery results

The associate editor coordinating the review of this manuscript and approving it for publication was Long Xu.

will still be exaggerated under uneven illumination, leading to excessive enhancement. Therefore, to overcome the shortcomings of HE, different kinds of the modifications such as contrast limit [6], weight adjustment [7], and brightness maintenance [8]–[10] have been developed.

Recently, researchers have begun to focus on methods based on decomposition models. Most of the algorithms are based on the Retinex theory [11], which assumes that the human eye scene is the product of the reflectance component and the illumination component. It means that the pixel intensity is the product of illuminance and reflectance. The traditional Retinex-based enhancement method is designed to separate the illumination layer from a given scene accurately. Usually, the estimated reflectance (or enhanced reflectance) component is used as the result of illumination invariance enhancement [12]–[16]. Although these algorithms can effectively emphasize the details of the image, the inappropriate decomposition between the illumination component and the reflectance component may cause visual discomfort [17]. According to the Retinex theory, it is unreasonable to treat the reflectance component only as an enhanced image [18].

Since most traditional histogram equalization methods strongly depend on setting parameters to achieve the optimal enhancement effect for different images. Also, the conventional decomposition of the reflectance component and the illumination component based on Retinex theory takes time for calculation. In this paper, a simple and effective image enhancement method is proposed. The illumination of each pixel is estimated by using an induced norm of a patch of the image. The computation time can be significantly reduced. A novel pre-gamma correction and a novel noise reduction method, all based on the local patch of an image, are proposed to improve the CLAHE processing and better visualize the input image. A novel post-gamma correction is proposed to enhance the dark regions of images slightly and not affect the brighter regions.

Recently, contemporary deep learning-based methods provide state-of-the-art performance for image enhancement tasks. Some methods based on neural networks have been proposed in the field of computer vision. Wang and Hu [19] proposed a multi-layer convolutional neural network that includes convolution kernels of different sizes for the three channels of the original images. The convolution kernel size is determined by calculating the mean square deviation of the pixels of the corresponding channel. The proposed algorithm can enhance weak contrast images with better details. Guo *et al*. [20] proposed a low-light image enhancement based on an end-to-end fully convolutional network and discrete wavelet transformation. The pipeline neural network consists of a denoising network and a low-light image enhancement network, which learns a function from a pair of dark and bright images. Guo *et al*. [21] proposed Zero-Reference Deep Curve Estimation (Zero-DCE), which trains a lightweight deep network, DCE-Net, to estimate pixel-wise and high-order curves for dynamic range adjustment of a given image. The method does not require any paired or unpaired data during training and is efficient for low-light image enhancement.

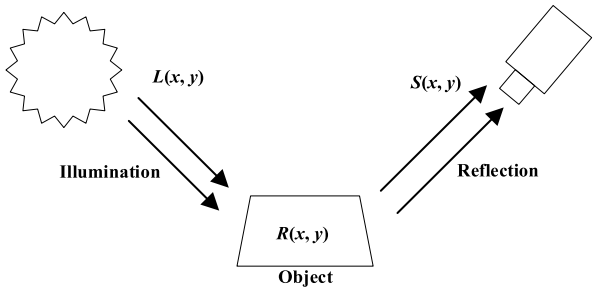


**FIGURE 1.** Illustration of Retinex theory.

The rest of this paper is organized as follows. Section II provides a brief survey of related work. Section III describes our proposed image enhancement. Section IV shows the experimental results to compare different methods and related analysis. Finally, concluding remarks are given in Section V.

## II. RELATED WORKS

In this section, we briefly introduce the image enhancement methods proposed in the field of computer vision. As mentioned earlier, the image contrast enhancement is mainly divided into two mainstream ideas: based on histogram equalization and based on the Retinex algorithm.

### A. RETINEX ALGORITHM

The Retinex algorithm [22] was first proposed by Edwin Land (1964). It first introduced human visual characteristics into the literature in the field of image enhancement research. When the human eye observes an object, its color is not just the spectral energy reflected by the object. The color perception is obtained by comparing the color and lightness value between this object and surrounding neighboring objects. The Retina and Cortex process this color perception ability in the human brain. In human vision, the stimulus value of the image is obtained by the retina (Retina). Then the color information obtained by the retina of the cerebral cortex (Cortex) is used to know the color of the object. In this way of operation, people can feel the real image. Fig. 1 shows the operation principle of Retinex.

Retinex is derived from the color constancy model of the human visual system [23]. Afterward, the model was extended to decompose the image $S$ into two different images, namely the reflectivity image $R$ and the illumination image $L$ as follows.

$$S(x, y) = R(x, y) \cdot L(x, y). \tag{1}$$

When the illumination is uneven, we only need to extract the illumination image $L(x, y)$ from the observation image $S(x, y)$, and then subtract $L(x, y)$ from $S(x, y)$. The real image $R(x, y)$ can be obtained. In the following, we briefly investigate different image enhancement algorithms based on the Retinex theory [24].

The Retinex theory assumes that the perception of color has a strong correlation with reflectivity. The amount of visible light that reaches the observer depends on the product of reflectivity and illuminance [25]. Most algorithms based on Retinex can enhance the details by eliminating the illumination to extract the reflectivity. However, it is impossible to remove the illumination for unsmooth depth scenes [12], [26]. In practice, the reflectance should be between 0 and 1, which means that the light reflected by the surface cannot exceed the light it receives. For example, 50% of the reflectance obtained by Single Scale Retinex is greater than one and may cause over-enhancement [27]. Furthermore, it is unreasonable to simply delete the necessary lighting that represents the environment [18].

Since the traditional Single-Scale Retinex (SSR) and multi-scale Retinex approaches often yield unnatural result [17], [28], Some approaches, such as intrinsic image decomposition [28], [29] and illumination map estimation [30], have been proposed to adjust the decomposed illumination component for image enhancement. However. Most traditional methods, including intrinsic image decomposition, require high computation to implement the model procedure and are hardly applied to mobile.

Kim [17] proposed the principal energy analysis based on the key observation that the illumination component is dominant over a small local region. The corresponding energy can be separated from the scene reflectance by exploiting the subspace analysis. The Singular Value Decomposition (SVD), which is useful for factorizing given data and revealing the underlying structure of their distribution [31], [32], was applied to estimate the illumination component by defining the small local patch at each pixel position and conduct the orthogonal transform for the corresponding region.

The SVD computational procedure is expressed as follows:

$$B(x, y) = USV^T, \tag{2}$$

where $S$ denotes the diagonal matrix and has the singular values as its diagonal term, i.e., $S = diag(s_1, s_2, \cdots, s_N)$, which represent the power of the independent component. $U$ and $V$ denote orthogonal matrices while satisfying $U^T U = I$ and $V^T V = I$. Therefore, the largest $s_1$ can be regarded as the principal energy related to the illumination component in the current pixel position.

Although the principal energy approach can obtain better decomposition results, the SVD computation still takes time. Since the largest $s_1$ obtained from SVD is equivalent to the Frobenius norm, which is just the norm 2 on a square matrix $B(x, y)$.

The Frobenius norm $\|\|_F$ is defined so that for every square $n \times n$ matrix $A \in M_n(\mathbb{C})$,

$$\|A\|_F = \left( \sum_{i,j=1}^{n} |a_{ij}|^{1/2} \right) = \sqrt{\mathrm{tr}(AA^*)} = \sqrt{\mathrm{tr}(A^*A)}. \tag{3}$$

In order to reduce the computation time and still obtain a better decomposition effect, a patch-based induced norm is proposed to estimate the illumination of images in this paper.

### B. NATURALNESS

Naturalness means that the overall atmosphere of the image should not be severely changed, and the direction of the light source should not be significantly changed. Recently, some natural enhancement algorithms [18], [33], [34] based on Retinex theory have been proposed to retain naturalness, but these algorithms may not be suitable for non-uniformly illuminated images [27].

### C. GAMMA CORRECTION

Huang *et al.* [35] employed a Compensated Cumulative Distribution Function (CDF) as an adaptive parameter, modifying the intensity with a progressive increment of the original trend. The proposed Adaptive Gamma Correction with Weighting Distribution (AGCWD) is formulated as follows:

$$T_{AGCWD}(l) = l_{\max}(l/l_{\max})^{1-cdf_\omega(l)}, \tag{4}$$

$$cdf_\omega(l) = \frac{\sum_{l=0}^{l} pdf_\omega(l)}{\sum_{l=0}^{l_{\max}} pdf_\omega(l)}, \tag{5}$$

$$pdf_\omega(l) = pdf_{\max}\left( \frac{pdf(l) - pdf_{\min}}{pdf_{\max} - pdf_{\min}} \right)^{\alpha}, \tag{6}$$

$$pdf(l) = \frac{n_l}{MN}, \tag{7}$$

where $n_l$ is the number of pixels in the gray level $l$, $MN$ is the total number of pixels of an image.

Several researchers have demonstrated that local correction can significantly improve image quality relative to a global correction [36]. Since the Gamma function only allows for the global contrast, a modified Gamma function based on local patches is proposed in this paper.

### D. HISTOGRAM EQUALIZATION

Contrast Enhancement (CE) technology has been widely used in various image enhancement applications. Histogram Equalization (HE) is one of the most popular and simple CE technologies [37]. HE uses the Probability Density Function (PDF) of the gray level of the input image to construct a cumulative distribution function and performs gray level mapping to redistribute the brightness histogram evenly so that the image is evenly distributed. This method can produce a good contrast enhancement effect on almost all images. However, there are serious problems, including unnatural effects or artifacts on images with high peaks in some histograms. Therefore, the degree of enhancement cannot be accurately controlled, which causes some visual degradation effects. For example, some areas of color images have a color shift and excessive enhancement.

Many histogram-based CE algorithms can use various methods to improve HE. For example, Bi-HE (BHE) is an algorithm that divides a histogram into two sub-histograms and applies HE to each sub-histogram [38]. Brightness-preserving Bi-Histogram Equalization (BBHE) uses the average intensity value of the input image to segment its histogram [39]. Brightness Preserving Dynamic Histogram Equalization (BPDHE) [10] first divides the

histogram into several sub-histograms, then applies HE to each sub-histogram separately, and then performs the normalization process. The contrast-enhanced image has the same average intensity value as the input image. These existing histogram-based CE methods tend to retain all average intensity values while improving the contrast of the entire image. There are other well-known methods to improve HE [40]–[42]. However, they are susceptible to parameters and only provide good image quality after careful parameter tuning.

At the same time, Adaptive Histogram Equalization (AHE) [43], [44] was developed, which is a CE using local statistical characteristics. AHE successfully considers local statistical properties, unlike traditional histogram equalization algorithms. AHE equalizes each pixel through a histogram of pixels within a rectangular range around it. The method of equalization is exactly the same as the HE algorithm. Therefore, the algorithm is more suitable for improving the local contrast of the image and obtaining more image details. However, AHE still has the problem of excessively magnifying the noise in the same area of the image. When the pixel values contained in a specific area are very similar, the histogram will be sharpened. At this time, the transformation function of the histogram will map a narrow range of pixels to the entire pixel range, which causes a small amount of noise in some flat areas to be excessively amplified. AHE does not consider the overall appearance of the image and has a high computation complexity.

Partially Overlapped Sub-block Histogram Equalization (POSHE) [45] and Cascaded Multistep Binomial Filtering HE (CMBFHE) [46] enhance AHE as a consideration of the overall appearance of the image and reduce the computational complexity. However, these methods are still computationally expensive, making them unusable for commercial use.

In order to solve the problem of excessive magnification, the method of Contrast Limited Adaptive Histogram Equalization (CLAHE) is used [47]. The difference between CLAHE and AHE is the contrast limiting. CLAHE uses the threshold value to cut the sharpened histogram and evenly distributes the cut parts to other histogram parts. This method improves the disadvantage that histogram equalization reduces the contrast in areas with moderate brightness when processing high-contrast or low-contrast images. It also improves the noise problem caused by adaptive histogram equalization for histogram sharpening. However, the disadvantage of this method is that it cannot be processed automatically. A threshold must be set for clipping, and this threshold will affect the quality of image processing.

The clip point is calculated as follows:

$$\beta = \frac{M}{N}\left(1 + \frac{\alpha}{100} S_{\max}\right), \tag{8}$$

where $M$ is the number of pixels in each block, $N$ is the dynamic range in this block, $S_{\max}$ is the maximum slope, and $\alpha$ is the clip factor. It is noted that the value of the clip factor $\alpha$ is to be determined based on the image being processed.

Based on the average gray value and standard deviation, which represent textures of a block, Chang *et al*. [48] set the clip point adaptively as follows:

$$\beta = \frac{M}{N}\left(1 + P\frac{l_{\max}}{R} + \frac{\alpha}{100}\left(\frac{\sigma}{Avg + c}\right)\right), \tag{9}$$

where $\sigma$ denotes the standard deviation of the block, $Avg$ denotes the mean value, and $c$ is a small value to avoid division by 0, $R$ represents the entire dynamic range of the image. $P$ and $\alpha$ are parameters to control the weights of the dynamic range and entropy terms, respectively. It should be noted that parameters $P$ and $\alpha$ are still to be determined, and different parameter values may have different image enhancement. Determining the parameter values will be a critical issue in getting a better image contrast enhancement for all types of low dynamic range images. In this paper, since all types of low dynamic range images are pre-processed by the pre-gamma correction function based on local patch, the parameters $\alpha$ for the clip point of CLAHE can be fixedly set as a small value and still achieve better image enhancement.

## III. PROPOSED METHOD

Most state-of-the-art techniques in image contrast enhancement might not be suitable for all types of low dynamic range images since different types of degraded images may require different enhancements. Hence, a new image enhancement method is proposed based on the statistical information of the respective images. The flowchart of the proposed method is shown in Fig. 2 and illustrated as follows.

Since the RGB color components are not decoupled, the RGB color model is not suitable for enhancement. In the HSV color model, the color content (V) intensity can be used to enhance the color image. Therefore, color space transformation is performed to convert the input image from RGB into HSV. The proposed image enhancement method is applied to the V component. The new proposed approach is based on the fact that the illumination component is dominant over a small region defined at each pixel position. A measure of the induced norm in the local patch provides a good approximation of the illumination component, which can be easy to implement in mobile devices. The estimated illumination is subsequently adjusted by a pre-Gamma function, CLAHE, noise reduction algorithm, and post-Gamma function, combined with the reflectance layer and $H$, $V$ components, and converted back to RGB image for generating the enhanced image.

### A. ILLUMINATION ESTIMATION VIA INDUCED NORM

The illumination component is estimated by defining a small local patch at each pixel position. The small local patch denoted as $B(x, y)$ of size $N \times N$ pixels is centered at $(x, y)$ pixel position, where $N$ is set to be 5. The procedure of estimating the illumination component is as follows:

The $L$-1 norm of $B(x, y)$ is defined as:

$$\left\|B(b_{ij})\right\|_1 = \max_j \sum\nolimits_{i=1}^{N} \left|b_{ij}\right|, \tag{10}$$

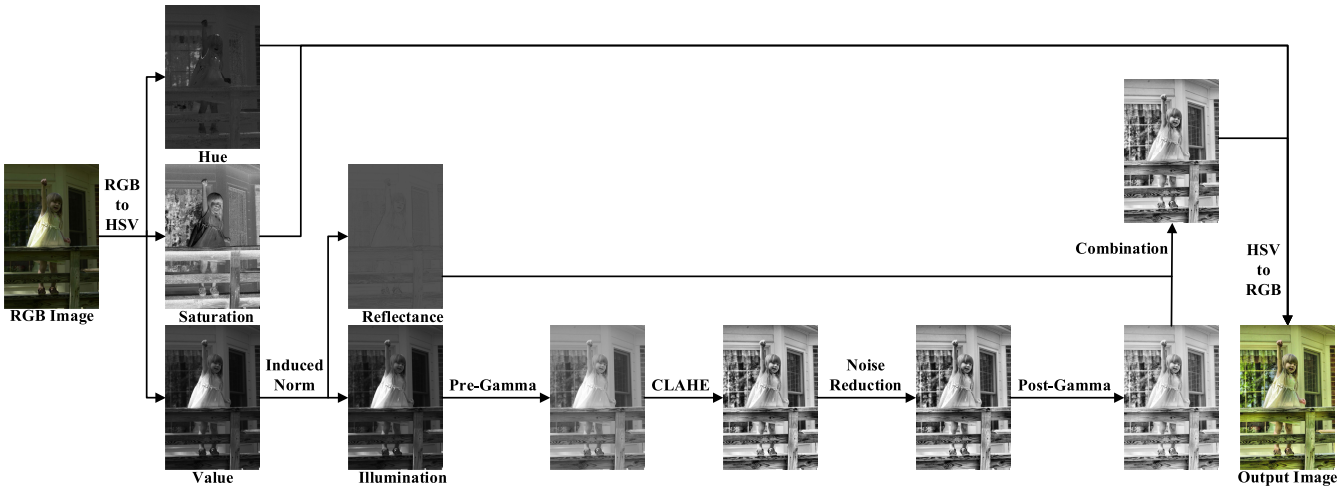


**FIGURE 2.** The flowchart of the proposed contrast enhancement method.


**FIGURE 3.** (a) Intensity channel of the original input image. (b) Estimated illumination map. (c) Estimated reflectance map.

The $L$-$\infty$ norm of $B(x, y)$ is defined as:

$$\left\|B(b_{ij})\right\|_{\infty} = \max_{i} \sum_{j=1}^{N} \left|b_{ij}\right|, \tag{11}$$

where $b_{ij}$ denotes the intensity of the pixel at location $(i, j)$.

Similar to the principal energy related to the illumination component, the illumination component in the current pixel position is estimated as:

$$i\,(x, y) = \max\left(\left\|B(b_{ij})\right\|_{1}, \left\|B(b_{ij})\right\|_{\infty}\right). \tag{12}$$

Compared with the principal energy approach, the proposed method can achieve better low computational costs.

An image can be defined as a two-dimensional function $f(x, y)$, where $x$ and $y$ are spatial coordinates, and the amplitude of $f$ is the intensity of the image at the point $(x, y)$. The intensity of the image $f(x, y)$ is a product of the illumination and reflectance components:

$$f\,(x, y) = i(x, y)\cdot r(x, y), \tag{13}$$

where $r(x, y)$ denotes the reflectance component.

The reflectance component $r(x, y)$ at each pixel position can be written as:

$$r\,(x, y) = f(x, y)/(i\,(x, y) + \varepsilon), \tag{14}$$

where $\varepsilon$ is a small positive number to avoid zero-division.

Fig. 3 shows the results of the illumination component and the reflectance component of an image. It is noteworthy that edges and textures, i.e., reflectance components, are well revealed even under unevenly lighted regions, for example, the dark window of the right side (see Fig. 3 (c)).

### B. IMAGE ENHANCEMENT BY PRE-GAMMA CORRECTION

An adaptive gamma correction based on local patch is proposed to pre-process all types of low dynamic range images enhance as follows:

$$I_{out} = I_{in}^{\gamma}, \tag{15}$$

$$\gamma\,(x, y) = \frac{(1-(\mu+\sigma)) \times e^{\left(-cdf_{WD}(I(x,y))\right)} + (\mu+\sigma)}{A(x, y)}, \tag{16}$$

$$A\,(x, y) = \frac{I\,(x, y)}{\frac{1}{N\times N}\sum_{(x,y)\in B} I\,(x, y)}, \tag{17}$$

where $I_{out}$, $I_{in}$, $\mu$ and $\sigma$ denote the input, the output, the mean value, and standard deviation of the image, respectively. The small local patch $B(x, y)$ of size $N \times N$ pixels is centered at $(x, y)$ pixel position, where $N$ is set to be 5. Since the image is processed based on a local patch, the local feature and naturalness can be preserved.

### C. IMAGE ENHANCEMENT BY CLAHE

The CLAHE limits the amplification by clipping the histogram at a predefined value before computing the CDF. The clip limit of CLAHE is the key parameter to adjust the contrast enhancement. Since the pre-gamma correction is applied to pre-process the images based on the local patch, the parameters $\alpha$ in (8) for the clip point of CLAHE can be set as a small value for all types of images. In this paper, each image is divide into $8 \times 8$ blocks. The proposed clip point for all types of low dynamic range images is calculated as follows:

$$\beta = \frac{M}{N}\left(1 + 0.004 S_{\max}\right). \tag{18}$$


**FIGURE 4.** (a) Without pre-processing noise before image enhancement. (b) With pre-processing noise before image enhancement.

### D. NOISE REDUCTION METHOD

Although CLAHE can improve the noise problem caused by adaptive histogram equalization for histogram sharpening, more or less noise may still exist in the image. A noise reduction algorithm is proposed to reduce noise from the image as follows:

$$I_{out} = I_{in}^{\gamma}, \tag{19}$$

$$\gamma(x,y) = \frac{e^{\left(\frac{\mu}{0.5}-1\right)}}{A(x,y)} \quad \text{for } \mu > 0.5, \tag{20}$$

$$\gamma(x,y) = 1 \quad \text{for } \mu \le 0.5, \tag{21}$$

where $I_{out}$, $I_{in,}$ and $\mu$ denote the input, the output, and the mean of the image intensity, respectively. Similarly, $A(x, y)$ is the same as that of (17), and the local noise of the image can be magnified.

After magnifying the noise, and the noise can be separated as follows:

$$I_{noise} = I_{out} - I_{in}. \tag{22}$$

The extracted noise is enhanced by noise characteristics, and the noise characteristics are adaptively enhanced according to the standard deviation $\sigma$ of the image, and the noise is removed by:

$$I_{out} = I_{in} - (I_{noise} \cdot (1+\sigma)). \tag{23}$$

It can be seen from Fig. 4(a) that noise appears after applying gamma correction without noise reduction processing. The noise of the image can be effectively reduced by using the proposed noise reduction processing, as shown in Fig. 4(b).

### E. IMAGE ENHANCEMENT BY POST-GAMMA CORRECTION

After applying CLAHE, the intensities of the image are scattered over the entire dynamic range, and brightness correction may become more critical than contrast enhancement. A post-gamma correction is proposed to adjust the brightness of the image as follows.

The final illumination adjustment based on the mean $\mu$ and standard deviation $\sigma$ of the image is shown as follows:

$$I_{out} = I_{in}^{\gamma}, \tag{24}$$

$$\gamma(x,y) = 1 - \left(I_{in}(x,y) - I_{in}(x,y)^{\omega}\right)^{\sigma}, \tag{25}$$

$$\omega = e^{\left(\frac{\mu}{0.5}-1\right)}, \tag{26}$$

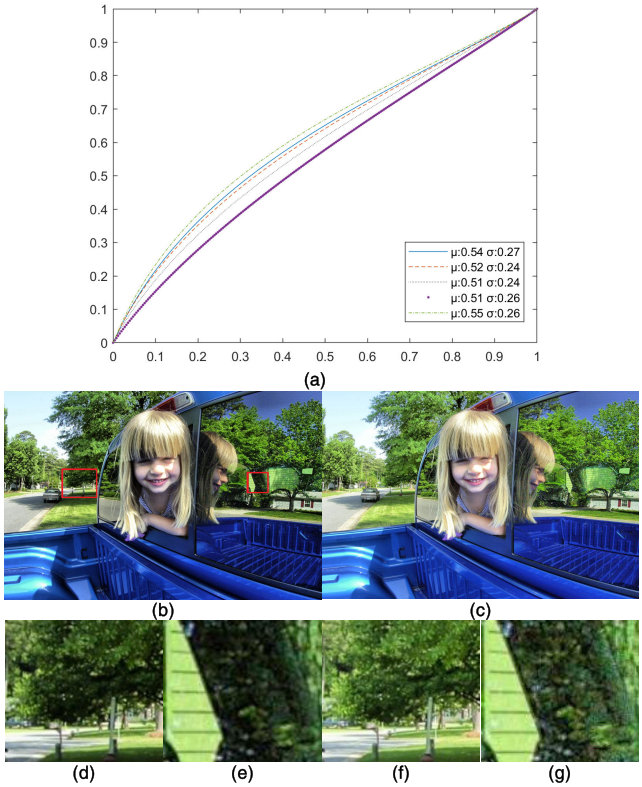


**FIGURE 5.** (a) Transformation curve for test images. (b) Image before post-gamma. (c) Image after post-gamma. (d)–(e) Detailed image information from enlarging (b) red block. (f)–(g) Detailed image information from enlarging (c) red block.

where $\omega$ is affected by $\mu$. Fig. 5(a) shows the transformation curves for different values of $\mu$and$\sigma$. It is noted that the values of $\mu$ of images after pre-gamma correction and CLAHE are mostly around 0.5∼0.6. It can be seen that the post-gamma correction only slightly enhances the dark regions of images and does not affect the brighter regions. Figs. 5(b)–(e) demonstrate that the dark regions become more visible after the post-gamma correction.

## IV. EXPERIMENTAL RESULTS

In this section, the test samples were taken from the NASA database [49], Hasinoff *et al.* [50], Guo *et al.* [30], and a small part of the images were searched by Google Images, which included backlight, cast shadows, uneven illumination, and low light. The proposed image enhancement method is evaluated based on 2,000 images obtained under various lighting conditions. The sizes of the test images are from 640 × 449 pixels to 8, 670 × 5.526 pixels. The traditional methods were implemented by using the codes with default parameters provided by the authors. The computer used in this experiment includes Intel Core i9-9900X CPU at 3.60GHz, 64GB RAM, and Matlab version 2020a. The details of the experimental results are explained in the following subsections.

### A. SUBJECTIVE COMPARISONS

In order to show the effectiveness of the proposed method, we use common images for comparison. Due to space

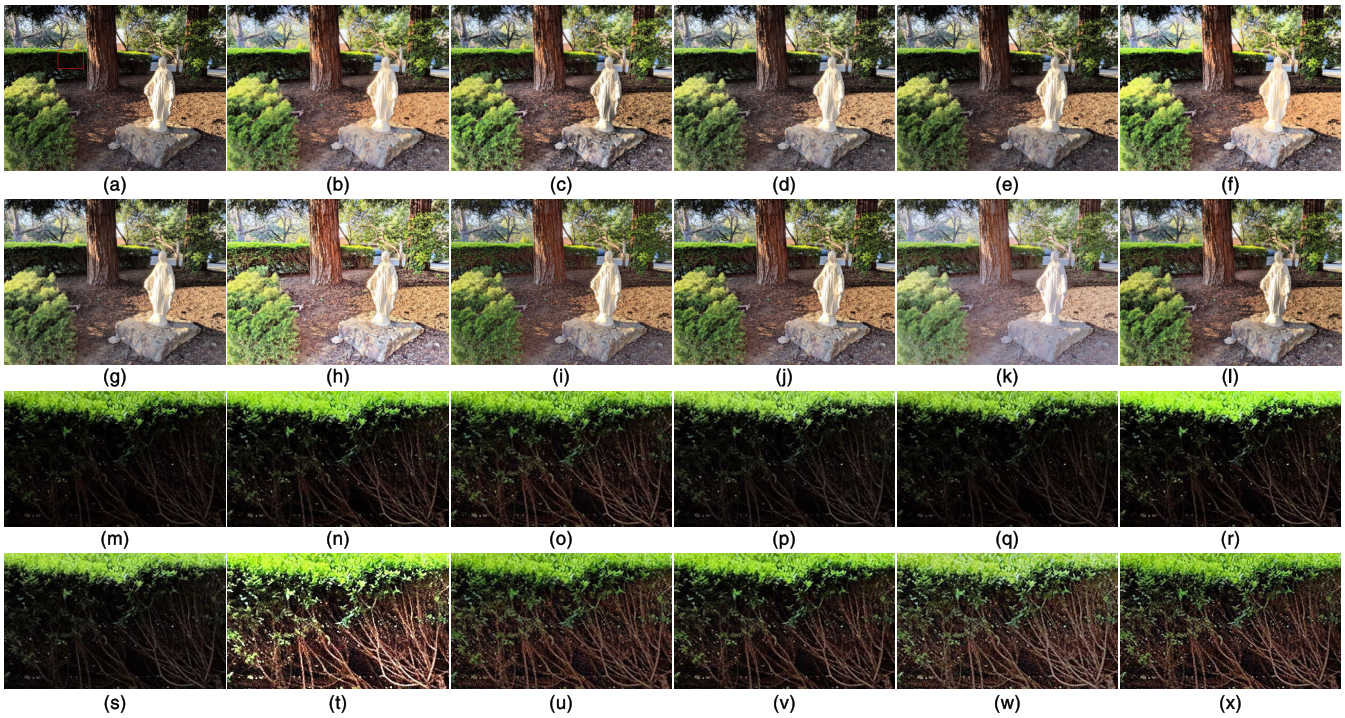


**FIGURE 6.** The visual comparison between image contrast enhancement results. (a) Original (b) HE (c) CLAHE (d) CVC (e) LDR (f) AGCWD (g) HMF (h) LIME (i) NPEA (j) WVM (k) Zero-DCE (l) ICEBIN. (m)–(x) Detailed image information from enlarging (a)–(l) red block.

limitations, the experiment in this section uses six images for experiment and image evaluation. Figs. 6–11 show some experimental results obtained by the proposed method and other state-of-the-art methods, which include HE, CLAHE, Contextual and Variational Contrast enhancement (CVC) [51], Layered Difference Representation (LDR) [52], AGCWD [35], Histogram Modification Framework (HMF) [53], Low-light image enhancement via Illumination Map Estimation (LIME) [30], Naturalness Preserved Enhancement Algorithm (NPEA) [27], histogram modification framework (WVM) [54], and Zero-Reference Deep Curve Estimation (Zero-DCE) [21], respectively.

Fig. 6(a) is an original photograph taken by the photography technique of sidelight. The light on the scene is very complex and produces uneven lighting. Because the lightness and darkness exist side by side and are overlapped, the subject will produce a more obvious shadow. It makes the outline of the subject more prominent and looks more three-dimensional, as shown in the statue on the right. As shown in Fig. 6(b), although the method of HE is simple, some of the details are lost (e.g., the details in the right area of the statue are less visible). It can be seen that CLAHE has better image enhancement effects than HE, as shown in Figs. 6(b) and 6(c). In Fig. 6(o), the dark area is less visible compared with the proposed method, as shown in Fig. 6(x). In Fig. 6(d), CVC shows some conservative results that cannot accurately enhance the clarity of content that belongs to dark areas. LDR is based on the traditional histogram method. The effect of image enhancement is not obvious, and there is not much difference in spatial light distribution from the original image, as indicated in Fig. 6(e). As shown in Fig. 6(f), although AGCWD can perform the effect of image enhancement, the effect of enhancement in dark areas is insufficient. The brightness of the statue is too high, making the outline of the statue inconspicuous. In Fig. 6(g), the effect of HMF in dark places is less visible. In Fig. 6(h), LIME shows the effect of excessive image enhancement. The overall image is overexposed, and the color saturation is very high, making the image unnatural. NPEA improves the low contrast displayed in the corresponding area, where the area of detail in the dark is less conspicuous, as indicated in Fig. 6(i). As shown in Fig. 6(j), WVM obtains better results in dark areas, but it still suffers from low contrast. In Fig. 6(k), Zero-DCE also obtains better results in dark areas, but the entire image is excessively enhanced. Fig. 6(l) shows that ICEBIN successfully prevents excessive enhancement of bright areas. ICEBIN can restore the texture details in dark areas and retain the color attributes and contrast of the original image. Figs. 6(m)–(x) respectively show the details of the dark areas which are obtained from enlarging the red block in the upper left corner of Fig. 6(a). It is worth noting that the sharpness of the shadow in the Figs. 6(n)–(s) cannot be shown. Fig. 6(t) shows that LIME can show the details in the shadows, but the entire image is excessively enhanced. The details in the shadow of Figs. 6(u)–(v) are not clear enough together with the loss of other details in the bright area. Fig. 6 (w) shows that Zero-DCE can show the details in the shadows, but the color saturation is insufficient (e.g., the tree on the left

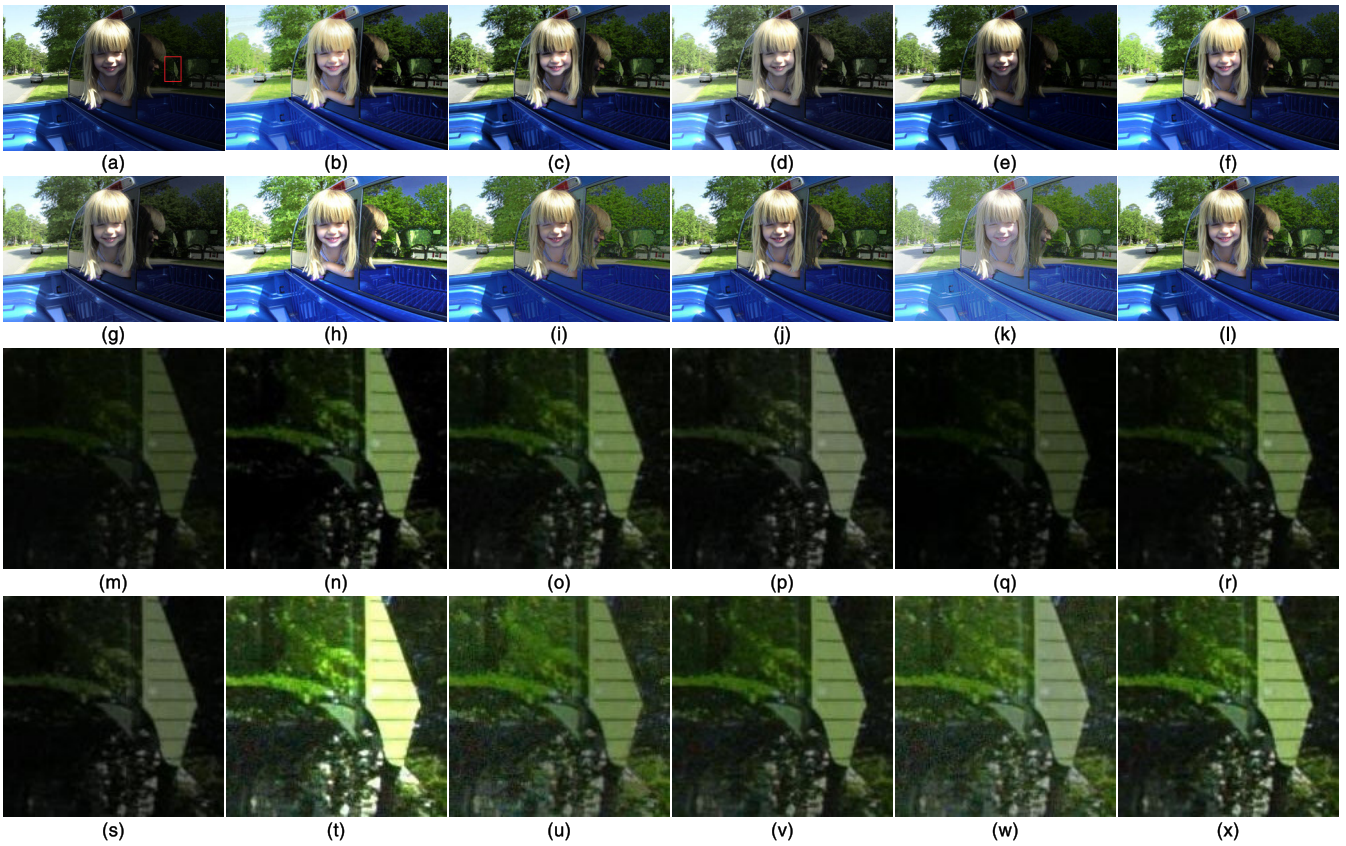


**FIGURE 7.** The visual comparison between image contrast enhancement results. (a) Original (b) HE (c) CLAHE (d) CVC (e) LDR (f) AGCWD (g) HMF (h) LIME (i) NPEA (j) WVM (k) Zero-DCE (l) ICEBIN. (m)–(x) Detailed image information from enlarging (a)–(l) red block.

in Fig. 6(k)). Compared with the state-of-arts method, the proposed method greatly restores the edges and texture of the dark area, as shown in Fig. 6(x). At the same time, the color attributes of the original input are maintained without greatly exaggerating the contrast.

The image in Fig. 7(a) is from the NASA database. The light in a given scene in the image is very complicated. Compared with Fig. 6(a), the image of Fig. 7(a) suffers more sidelight. Therefore, this uneven illumination will easily lead to the unbalanced image enhancement processed by the previous models such as HE, CLAHE, CVC, and LDR. In Fig. 7(b), HE is a traditional histogram-based method, suitable for uniformly dark or bright images. However, for uneven illumination images, satisfactory results will not be produced. Figs. 7(c)–(e) show that the contrast enhancement performance of CLAHE, CVC, and LDR in low-light environments is limited. Fig. 7(f) shows that although AGCWD can achieve better image enhancement, the details reflected on the window are not visible. Fig. 7(g) shows that HMF cannot increase the brightness properly, and the original color of the image is also decreased. Fig. 7(h) shows that LIME successfully reveals the underlying structure reflected on the window. However, there is an excessive enhancement in the bright areas of the image, such as the image of the tree on the left of the picture. Fig. 7(i) shows that NPEA over-enhances the image, where some details of the image are lost, and noise and color deviation are increased. Fig. 7(j) shows that WVM is good at preserving the naturalness of the image. However, the dark area is not clear enough. For example, the area reflected on the window is less visible. Fig. 7(k) shows that the Zero-DCE image enhancement is unbalanced, resulting in a white appearance. The original color attribute of the image cannot be maintained. In Fig. 7(l), the proposed method provides almost the same quality in the bright areas as the original image. For example, the tree on the left of the picture is not over-enhanced. The entire image is not overexposed, and the outline of the object is clear, making the image look natural. Figs. 7(m)–(x) respectively show the details of the shadows reflected on the window, which are obtained from enlarging the red block on the right side of Figs. 7(a)–(l). Figs. 7(n)–(s) cannot accurately restore the brightness and sharpness of the shaded area within the red block. Fig. 7(t) LIME can restore the contents of the dark place but enhances the image too much such that details cannot be presented. In Fig. 7(u), NPEA results in an image with low color saturation. Also, it can be seen from the enlarged image that there is too much image noise. Fig. 7(v) shows that the details of the dark area of WVM are not clear enough from the enlarged image. Fig. 7(w) shows that although Zero-DCE has enhanced the brightness of the dark area, the color properties are different


**FIGURE 8.** The visual comparison between image contrast enhancement results. (a) Original (b) HE (c) CLAHE (d) CVC (e) LDR (f) AGCWD (g) HMF (h) LIME (i) NPEA (j) WVM (k) Zero-DCE (l) ICEBIN. (m)–(x) Detailed image information from enlarging (a)–(l) red block.

from those of the original image. As shown in Fig. 7(x), the proposed method shows that the overall image is not overexposed, and the image is obviously more natural. Also, dark areas have less noise than those of NPEA, and the edges and texture details in dark areas are clearer than those of WVM. Overall, ICEBIN achieves a good balance between detail enhancement and noise suppression.

Similar to the above description about Figs. 6(b)–(g) and 7(b)–(g), Figs. 8(b)–(g) and 9(b)–(g) show that the image enhancement effects are not obvious by using state-of-the-art methods. From the zoomed images in Figs. 8 (n)–(s) and 9(n)–(s), It is more obvious that the proposed method can achieve better enhancement results than the state-of-the-art methods. For example, it can be seen from Figs. 8(b) and 9(b) that HE causes some of the detail loss. CLAHE, CVC, and LDR cannot effectively enhance dark areas, as shown in Figs. 8(c)–(e) and 9(c)–(e), respectively. AGCWD converts most of the intensity to the white range ([128, 255]), where the image brightness exceeds expectations. For example, the details of the skirt in Fig. 9(r) disappear. HMF cannot properly increase the brightness, and the original tone of the image is also decreased, as shown in Fig. 9(g). Although the image enhancement effects, as shown in Figs. 8(h)–(k) and 9(h)–(k) are obvious, the quality of the results is still insufficient, which can be seen from the zoomed image in Figs. 8(t)–(w) and 9(t)–(w). For example, LIME shows an impressive performance in dark areas. However, it makes the brightness too saturated because it tends to over-enhance the relatively high-intensity area, such as the pillar in the middle of Fig. 8(h) and the skirt of Fig. 9(t). In contrast, ICEBIN produces more natural results while successfully enhancing the visibility of low-light images. NPEA is very effective when dealing with smaller size images. However, as the image size increases, the smoothness of the illumination deteriorates. This drawback causes the blurred appearance of the enhanced image in Figs. 8(i) and 8(u), especially in Fig. 9(i). WVM obtains good results in dark areas, but this method still encounters insufficient image enhancement. It can be seen that ICEBIN has a better image enhancement effect in Fig. 8(l) by comparing with Fig. 8(j). Zero-DCE attempts to stretch the narrow histogram of the dark image to enhance the contrast but makes the image over-enhanced and unnatural, as shown in Figs. 8(k) and 9(k). In general, ICEBIN can achieve a better image enhancement effect either for the full image shown in Figs. 8(l) and 9(l) or for the enlarged image in Figs. 8(x) and 9(x), but the state-of-the-art methods cannot.

Figs. 10–11 show the enhancement results of underlit indoor images with strong noise. It can be seen that the hidden noise is high under very weak lighting conditions, as shown in Figs. 10(a) and 11(a). In Figs. 10(c)–(g), the background of roses is less visible, and only Figs. 10(b) and 10(h)–(k) can

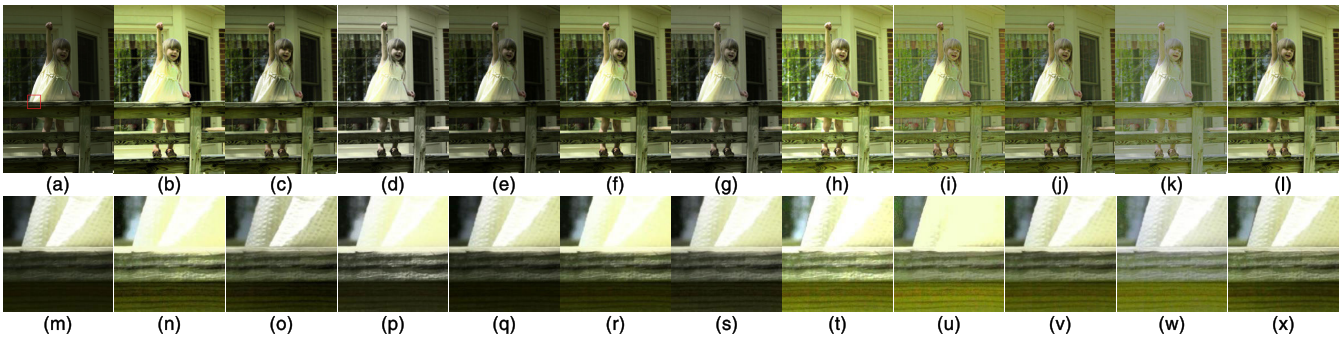


**FIGURE 9.** The visual comparison between image contrast enhancement results. (a) Original (b) HE (c) CLAHE (d) CVC (e) LDR (f) AGCWD (g) HMF (h) LIME (i) NPEA (j) WVM (k) Zero-DCE (l) ICEBIN. (m)–(x) Detailed image information from enlarging (a)–(l) red block.

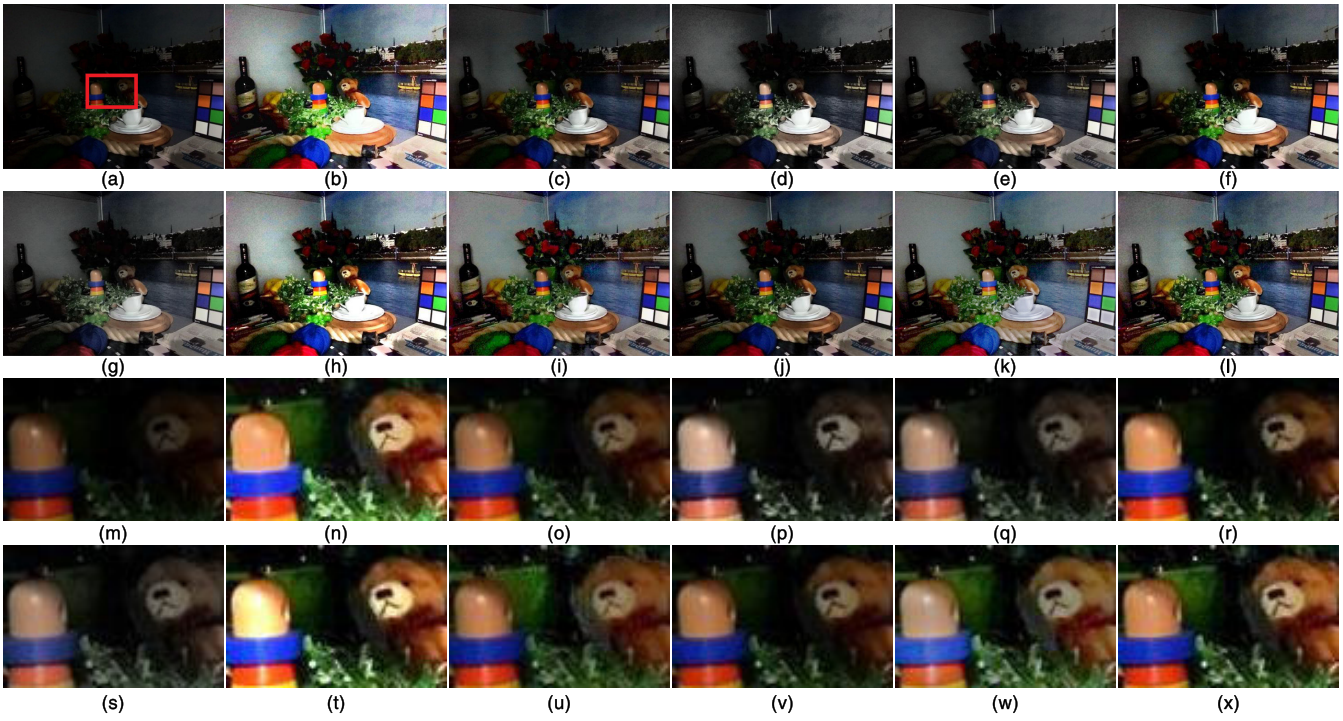


**FIGURE 10.** The visual comparison between image contrast enhancement results. (a) Original (b) HE (c) CLAHE (d) CVC (e) LDR (f) AGCWD (g) HMF (h) LIME (i) NPEA (j) WVM (k) Zero-DCE (l) ICEBIN. (m)–(x) Detailed image information from enlarging (a)–(l) red block.

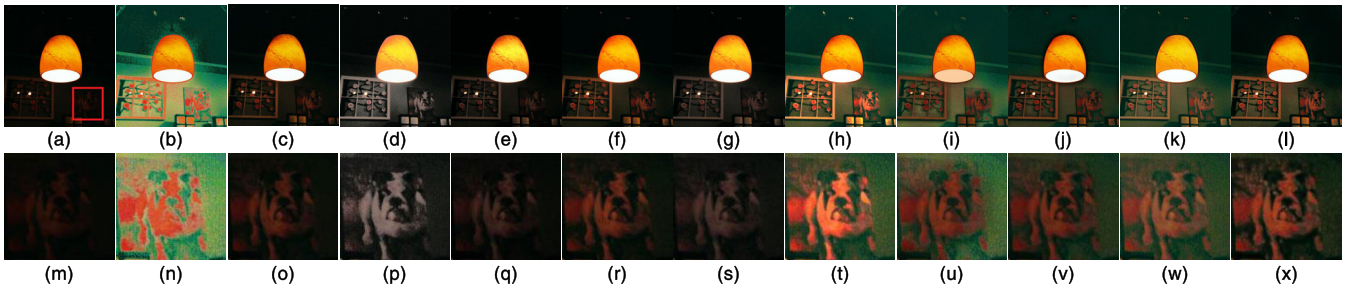


**FIGURE 11.** The visual comparison between image contrast enhancement results. (a) Original (b) HE (c) CLAHE (d) CVC (e) LDR (f) AGCWD (g) HMF (h) LIME (i) NPEA (j) WVM (k) Zero-DCE (l) ICEBIN. (m)–(x) Detailed image information from enlarging (a)–(l) red block.

show it. Moreover, the flower pot located in the middle of the enlarged Figs. 10(o)–(s) and 10(v) are invisible, and only Figs. 10(n), 10(t)–(u) and 10(w) –(x) can show it. Although HE and LIME can enhance the visibility of low-light images,

they cause the cup too high brightness, as shown in the middle of Figs. 10(b) and 10(h). NPEA results in the amplified noise in Fig. 10(u), and Zero-DCE has the loss of the original color in Fig. 10(w). The result of WVM is shown in Fig. 10(j). It can be seen that the content in the background has been successfully restored, but the color of the rose is still very dark. ICEBIN has satisfactory performance and can handle low-light images with strong noise, as shown in Fig. 10(l).

Similarly, Figs. 11(c) and 11(e)–(g) are unable to clearly show the painting of the dog on the right of the figure, but it can be clearly seen in Figs. 11(b), 11(d), and 11(h)–(l). From the enlarged images, the paintings of the dog are less visible in Figs. 11(o) and 11(q)–(s). Figs. 11(n), 11(p), and 11(t)–(x) show the pattern of the dog clearly. However, HE and NPEA tend to enhance noise and produce many false minute details as shown in Figs. 11(n) and 11(u). LIME over-enhances the input image in Fig. 11(t), especially in areas with higher illumination. Zero-DCE can enhance low-light and high-noise images in more detail than state-of-the-art methods, but the original color attribute cannot be maintained in the enhanced image (e.g., the lamp in the middle of Fig. 11 (k)). Although WVM can restore most of the content of the image in Fig. 11(j), ICEBIN can restore the details more clearly than the WVM by comparing Figs. 11(x) with 11(v). Overall, ICEBIN achieves a good balance between detail enhancement and noise suppression.

### B. OBJECTIVE QUALITY ASSESSMENTS

In addition to subjective assessment, we also objectively compare the proposed method with the state-of-the-art methods mentioned above. Since there is no objective standard like the human visual system, seven objective indicators widely used in visual quality metric are adopted, including Blind/Referenceless Image Spatial Quality Evaluator (BRISQUE) [55], Feature SIMilarity index (FSIM) [56], Measure of Enhancement (EME) [57], Colorfulness-based Patch-based Contrast Quality Index (CPCQI) [58], Naturalness Image Quality Evaluator (NIQE) [59], and Peak Signal-to-Noise Ratio (PSNR) to evaluate the special characteristics of enhanced images. BRISQUE measures the naturalness of the image based on the measurement deviation from the natural image model, which is based on natural scene statistical data. BRISQUE indicates the loss of naturalness of the image that may be caused by distortion. The higher the score is, the worse the image quality is. FSIM compares the structural and feature similarity between the enhanced result and the original image. EME is an image quality indicator that is more in line with the human visual system. The larger EME value corresponds to better image quality. The image is divided into multiple sub-image blocks. The average ratio of the maximum and minimum intensities in the image block evaluates the effect of image enhancement. The higher the enhancement is, the more obvious the enhancement effect is. CPCQI is an extended version of PCQI, taking the influence of color into consideration. CPCQI evaluates the degree of color distortion after enhancement by calculating the average intensity, gray level change and structural distortion between the original image and the enhanced result. NIQE evaluates image quality by measuring the distance between model statistics extracted from natural images and statistics of deformed images. NIQE works based on the quality perception set of the Natural Scene Statistics model, which can provide the perceived quality of a given image. PSNR is a ratio between the maximum possible power of a signal and the power of destructive noise that affects its accuracy. The high PSNR score represents the effective reconstruction of the image; the low the score represents the more serious of the distortion after reconstruction.

**TABLE 1. Objective quality assessments of enhanced results based on different methods.**

| | BRISQUE↓ | NIQE↓ | EME↑ | CPCQI↑ | FSIM↑ | PSNR↑ | Total Rank score |
|---|---|---|---|---|---|---|---|
| Original | 27.37 | 2.78 | 20.80 | 1.00 | 1.00 | - | - |
| HE | 26.69 (7) | 2.81 (6) | 19.82 (3) | 0.86 (9) | 0.92 (9) | 20.39 (4) | 38 |
| CLAHE | 25.10 (6) | 2.87 (7) | 19.60 (4) | 0.92 (2) | 0.94 (4) | 22.09 (3) | 26 |
| CVC | 27.04 (8) | 2.98 (9) | 25.92 (1) | 0.87 (6) | 0.92 (8) | 17.57 (9) | 41 |
| LDR | 31.55 (11) | 3.11 (11) | 19.85 (2) | 0.86 (8) | 0.98 (1) | 25.31 (1) | 34 |
| AGCWD | 29.07 (10) | 2.94 (8) | 18.48 (6) | 0.82 (10) | 0.94 (6) | 18.00 (8) | 48 |
| HMF | 28.43 (9) | 3.00 (10) | 16.55 (9) | 0.87 (7) | 0.97 (2) | 22.67 (2) | 39 |
| LIME | 19.90 (1) | 2.72 (1) | 17.48 (8) | 0.92 (3) | 0.86 (11) | 12.94 (11) | 35 |
| NPEA | 23.32 (3) | 2.76 (4) | 16.30 (10) | 0.89 (5) | 0.92 (7) | 18.17 (7) | 36 |
| WVM | 25.07 (5) | 2.73 (3) | 17.52 (7) | 0.89 (4) | 0.94 (5) | 18.64 (6) | 30 |
| Zero-DCE | 23.38 (4) | 2.80 (5) | 14.83 (11) | 0.82 (11) | 0.88 (10) | 14.16 (10) | 51 |
| ICEBIN | 21.81 (2) | 2.73 (2) | 19.02 (5) | 0.93 (1) | 0.95 (3) | 20.25 (5) | 18 |

Table 1 shows the results of the objective quality assessment of seven objective indicators for the original image and the images generated by nine contrast enhancement methods. In the table, the result of objective analysis for each method uses a number in brackets to indicate the ranking in the objective analysis. The number 1 stands for the highest score and number 11 for the lowest score. The final ranking score for each method in the rightmost column is the sum of all rankings.

It can be observed that, in terms of BRISQUE, the score of ICEBIN is only slightly larger than that of LIME, but the LIME result is excessively enhanced. For example, the color of the toy on the left side of Fig. 10(t) is over-enhanced, causing the color to become less visible. For NIQE, the score of ICEBIN is slightly larger than those of LIME and WVM, but the score is nearly similar. Also, ICEBIN has better scores than WVM in all other objective quality assessments. Moreover, it can be seen that the detailed processing of ICEBIN is more obvious than that of WVM in comparison with Figs. 6(v) and 6(x). EME divides the image into

multiple blocks, calculates the score based on the minimum and maximum gray levels in each block, and takes the average score to approximate the average contrast in the image. It can be seen that HE, CLAHE, CVC, and LDR provide better scores of EME. Unfortunately, compared with the original image, the enhanced colors look unnatural, as illustrated in the above section. It is worth noting that CPCQI will measure the perceived distortion based on the average strength of the local area, signal strength, signal structure, and color saturation. ICEBIN achieves the highest CPCQI score, which shows that ICEBIN achieves a good balance between detail enhancement and artifact suppression compared with other contrast enhancement methods. Among the evaluation methods of FSIM, the scores of LDR and HMF are relatively high. However, the performance of the proposed method in CPCQI is much higher than those of LDR and HMF, which means that LDR and HMF have higher color distortion. Although in PSNR, HE, CLAHE, LDR, HMF scores are higher than ICEBIN. But from a subjective view, the image enhancement effect of these four methods is not as good as ICEBIN.

BRISQUE and NIQE emphasize the naturalness of the image; CPCQI emphasizes the color distortion of the image; FSIM emphasizes the similarity of structure and feature of the image; and so on. The results of the subjective and objective experiments show that ICEBIN can effectively obtain the visual characteristics of the target image of the natural scene, suppress the interference and influence of useless information, and map the visual characteristics information more realistically. It should be noted that CLAHE has better image enhancement effects than HE when processing low-contrast images. It is worth noting that compared with the neural network enhancement algorithm (Zero-DCE), ICEBIN in overall performance (including subjective and objective comparison) is better than Zero-DCE. The results show that although the use of neural networks for image enhancement is popular recently, ICEBIN performance is superior. While completing feature mapping, ICEBIN can effectively maintain the original structure of the scene and achieve better subjective and objective effects than the state-of-the-art feature mapping algorithms. It can be seen that our method (ICEBIN) has a total score of 18, which is the highest-ranking among all methods. However, objective evaluation methods do not necessarily represent the quality of the image. Sometimes the human eye must be used to assist in judging the quality of the image.

### C. TIME ASSESSMENTS

We also evaluate the average processing time of all methods mentioned above. The source code of state-of-the-art methods can be found on the website of authors (provided as Matlab code) and can be directly used for performance comparison without any modification.

Matlab is used to evaluate processing time for fair performance comparison. Since the conventional Retinex method requires SVD calculation at each pixel position, it requires more processing time than CVC, LDR, and LIME. In order to improve the computation speed of the proposed algorithm and to speed up the calculation, the induced norm approach is proposed in this paper. In Table 2, we compare the performance by using various common image sizes 8K ($7,680\times4.320$), 4K ($3,840\times2.160$), Full HD ($1,920\times1.080$), HD ($1,280\times720$), SD ($720\times480$ pixels).

**TABLE 2.** Compare the processing time (second) of traditional SVD and ICEBIN induced norm.

| Image size | SVD | ICEBIN Induced Norm |
|---|---|---|
| 8K | 577.11 | 1.70 |
| 4K | 155.49 | 0.57 |
| Full HD | 35.31 | 0.15 |
| HD | 13.39 | 0.09 |
| SD | 4.88 | 0.02 |

**TABLE 3.** Compare the calculation time (second) of different methods.

| | HE | CLAHE | CVC | LDR | AGCWD | HMF | LIME | NPEA | WVM | ICEBIN |
|---|---|---|---|---|---|---|---|---|---|---|
| 8K | 4.56 | 5.21 | 11.47 | 5.12 | 2.72 | 4.29 | 11.23 | 741.45 | 807.24 | 6.22 |
| 4K | 1.29 | 1.44 | 3.05 | 1.30 | 0.60 | 1.19 | 2.80 | 182.55 | 172.19 | 1.60 |
| F.HD | 0.29 | 0.34 | 0.75 | 0.34 | 0.14 | 0.29 | 0.68 | 45.76 | 22.84 | 0.46 |
| HD | 0.15 | 0.16 | 0.35 | 0.19 | 0.06 | 0.15 | 0.30 | 20.17 | 9.94 | 0.17 |
| SD | 0.08 | 0.09 | 0.16 | 0.10 | 0.02 | 0.08 | 0.12 | 7.59 | 3.90 | 0.09 |
| AVG. | 1.27 | 1.45 | 3.16 | 1.41 | 0.71 | 1.20 | 3.03 | 199.5 | 203.22 | 1.71 |

It can be seen from Table 2 that the proposed induced norm can effectively shorten the calculation time. Among them, the 8K image is used as the test image for the computation time. The proposed method using the induced norm is about 339 times faster than the SVD and can effectively save the calculation time.

Table 3 shows the average computing time for different image sizes. The state-of-the-art methods, including HE, CLAHE, CVC, LDR, AGCWD, HMF, LIME, NPEA, WVM, and ICEBIN are listed in the horizontal row. It is noted that since Zero-DCE is executed in a Python environment, it is different from the execution environment of the other ten methods. For a fair comparison, the execution time of Zero-DCE is not listed in Table 3 for comparison. Different image sizes and the average computation time of each method are listed in the vertical columns. It can be seen from Table 3 that although the computation times of HE, LDR, AGCWD, and HMF are shorter than that of ICEBIN, because their algorithms are simple and the effects are limited. Overall, both experiments of Subjective Comparisons or Objective Quality Assessments show that the effects of the image contrast enhancement of the proposed method can achieve better performance. NPEA not only tends to generate noise in the image but also takes a long time for calculation. WVM has the longest computation time in Table 3. In comparison, the proposed method is approximately 118 times faster than WVM. The proposed method not only obtains better results in image enhancement but also has a better advantage under the computation speed consideration.

## V. CONCLUSION

In this paper, a simple and effective image enhancement method is proposed. The illumination of each pixel is estimated by using an induced norm of a patch of the image. The computation time can be significantly reduced. A novel pre-gamma correction and a novel noise reduction method, which are all based on the local patch of an image, are proposed to improve the CLAHE processing and achieve a better visual quality of the input image. A novel post-gamma correction is proposed to slightly enhance the dark regions of images and not to affect the brighter regions. With the novel pre-gamma correction and the novel noise reduction method, which are all based on the local patch of an image, the local feature and naturalness of images can be preserved. ICEBIN can automatically perform image enhancement for all types of low dynamic range mages without presetting its processing parameter values. Experimental image enhancement results demonstrate that ICEBIN performs well compared with other state-of-the-art methods. According to the analysis of time consumption, ICEBIN can be implemented in a mobile device with limited resources. ICEBIN is currently suitable to solve the problem of images with backlight, cast shadows, uneven illumination, or low light but unable to resolve haze images. Since de-haze algorithms are different from our ICEBIN, we will study de-haze algorithms in future work.

## REFERENCES


[1] P. E. Debevec and J. Malik, "Recovering high dynamic range radiance maps from photographs," in *Proc. ACM SIGGRAPH Classes*, New York, NY, USA, 2008, pp. 369–378.

[2] T. Mitsunaga and S. K. Nayar, "Radiometric self calibration," in *Proc. IEEE Comput. Soc. Conf. Comput. Vis. Pattern Recognit.*, Fort Collins, CO, USA, 1999, pp. 374–380.

[3] M. A. Robertson, S. Borman, and R. L. Stevenson, "Estimation-theoretic approach to dynamic range enhancement using multiple exposures," *J. Electron. Imag.*, vol. 12, no. 2, pp. 219–228, Apr. 2003.

[4] S. B. Kang, M. Uyttendaele, S. Winder, and R. Szeliski, "High dynamic range video," *ACM Trans. Graph.*, vol. 22, no. 3, pp. 319–325, 2003.

[5] E. Reinhard, W. Heidrich, P. Debevec, S. Pattanaik, G. Ward, and K. Myszkowski, *High Dynamic Range Imaging: Acquisition, Display, and Image-Based Lighting*. Burlington, MA, USA: Morgan Kaufmann, 2010, pp. 91–117.

[6] C. Li, J. Liu, A. Liu, Q. Wu, and L. Bi, "Global and adaptive contrast enhancement for low illumination gray images," *IEEE Access*, vol. 7, pp. 163395–163411, 2019.

[7] S.-H. Yun, J. H. Kim, and S. Kim, "Contrast enhancement using a weighted histogram equalization," in *Proc. IEEE Int. Conf. Consum. Electron. (ICCE)*, Jan. 2011, pp. 203–204.

[8] C. Wang and Z. Ye, "Brightness preserving histogram equalization with maximum entropy: A variational perspective," *IEEE Trans. Consum. Electron.*, vol. 51, no. 4, pp. 1326–1334, Nov. 2005.

[9] S. F. Tan and N. A. M. Isa, "Exposure based multi-histogram equalization contrast enhancement for non-uniform illumination images," *IEEE Access*, vol. 7, pp. 70842–70861, 2019.

[10] H. Ibrahim and N. Pik Kong, "Brightness preserving dynamic histogram equalization for image contrast enhancement," *IEEE Trans. Consum. Electron.*, vol. 53, no. 4, pp. 1752–1758, Nov. 2007.

[11] E. H. Land, "The retinex theory of color vision," *Sci. Amer.*, vol. 237, no. 6, pp. 108–129, 1977.

[12] D. J. Jobson, Z. Rahman, and G. A. Woodell, "Properties and performance of a center/surround retinex," *IEEE Trans. Image Process.*, vol. 6, no. 3, pp. 451–462, Mar. 1997.

[13] D. J. Jobson, Z. Rahman, and G. A. Woodell, "A multiscale retinex for bridging the gap between color images and the human observation of scenes," *IEEE Trans. Image Process.*, vol. 6, no. 7, pp. 965–976, Jul. 1997.

[14] M. Herscovitz and O. Yadid-Pecht, "A modified multi scale retinex algorithm with an improved global impressionof brightness for wide dynamic range pictures," *Mach. Vis. Appl.*, vol. 15, no. 4, pp. 220–228, Oct. 2004.

[15] Z.-U. Rahman, D. J. Jobson, and G. A. Woodell, "Retinex processing for automatic image enhancement," *J. Electron. Imag.*, vol. 13, no. 1, pp. 100–110, 2004.

[16] C. Xiao and Z. Shi, "Adaptive bilateral filtering and its application in retinex image enhancement," in *Proc. 7th Int. Conf. Image Graph.*, Qingdao, China, Jul. 2013, pp. 45–49.

[17] W. Kim, "Image enhancement using patch-based principal energy analysis," *IEEE Access*, vol. 6, pp. 72620–72628, 2018.

[18] B. Li, S. Wang, and Y. Geng, "Image enhancement based on retinex and lightness decomposition," in *Proc. 18th IEEE Int. Conf. Image Process.*, Brussels, Belgium, Sep. 2011, pp. 3417–3420.

[19] J. Wang and Y. Hu, "An improved enhancement algorithm based on CNN applicable for weak contrast images," *IEEE Access*, vol. 8, pp. 8459–8476, 2020.

[20] Y. Guo, X. Ke, J. Ma, and J. Zhang, "A pipeline neural network for low-light image enhancement," *IEEE Access*, vol. 7, pp. 13737–13744, 2019.

[21] C. Guo, C. Li, J. Guo, C. C. Loy, J. Hou, S. Kwong, and R. Cong, "Zero-reference deep curve estimation for low-light image enhancement," in *Proc. IEEE/CVF Conf. Comput. Vis. Pattern Recognit. (CVPR)*, Jun. 2020, pp. 1780–1789.

[22] E. H. Land, "The Retinex," *Amer. Sci.*, vol. 52, no. 2, pp. 247–264, 1964.

[23] E. H. Land, "Recent advances in retinex theory," *Vis. Res.*, vol. 26, no. 1, pp. 7–21, Jan. 1986.

[24] E. H. Land and J. J. McCann, "Lightness and retinex theory," *J. Opt. Soc. Amer.*, vol. 61, no. 1, pp. 1–11, 1971.

[25] M. Bertalmío, V. Caselles, and E. Provenzi, "Issues about retinex theory and contrast enhancement," *Int. J. Comput. Vis.*, vol. 83, no. 1, pp. 101–119, Jun. 2009.

[26] G. Deng, "A generalized unsharp masking algorithm," *IEEE Trans. Image Process.*, vol. 20, no. 5, pp. 1249–1261, May 2011.

[27] S. Wang, J. Zheng, H.-M. Hu, and B. Li, "Naturalness preserved enhancement algorithm for non-uniform illumination images," *IEEE Trans. Image Process.*, vol. 22, no. 9, pp. 3538–3548, Sep. 2013.

[28] H. Yue, J. Yang, X. Sun, F. Wu, and C. Hou, "Contrast enhancement based on intrinsic image decomposition," *IEEE Trans. Image Process.*, vol. 26, no. 8, pp. 3981–3994, Aug. 2017.

[29] J. Shen, X. Yang, X. Li, and Y. Jia, "Intrinsic image decomposition using optimization and user scribbles," *IEEE Trans. Cybern.*, vol. 43, no. 2, pp. 425–436, Apr. 2013.

[30] X. Guo, Y. Li, and H. Ling, "LIME: Low-light image enhancement via illumination map estimation," *IEEE Trans. Image Process.*, vol. 26, no. 2, pp. 982–993, Feb. 2017.

[31] J. Stander, R. Mech, and J. Ostermann, "Detection of moving cast shadows for object segmentation," *IEEE Trans. Multimedia*, vol. 1, no. 1, pp. 65–76, Mar. 1999.

[32] W. Zhang, X. Zhong Fang, and Y. Xu, "Detection of moving cast shadows using image orthogonal transform," in *Proc. 18th Int. Conf. Pattern Recognit. (ICPR)*, Hong Kong, 2006, pp. 626–629.

[33] S. Chen and A. Beghdadi, "Natural rendering of color image based on retinex," in *Proc. 16th IEEE Int. Conf. Image Process. (ICIP)*, Cairo, Egypt, Nov. 2009, pp. 1813–1816.

[34] S. Chen and A. Beghdadi, "Natural enhancement of color image," *EURASIP J. Image Video Process.*, vol. 2010, pp. 1–19, Dec. 2010.

[35] S.-C. Huang, F.-C. Cheng, and Y.-S. Chiu, "Efficient contrast enhancement using adaptive gamma correction with weighting distribution," *IEEE Trans. Image Process.*, vol. 22, no. 3, pp. 1032–1041, Mar. 2013.

[36] C. Li, S. Tang, J. Yan, and T. Zhou, "Low-light image enhancement via pair of complementary gamma functions by fusion," *IEEE Access*, vol. 8, pp. 169887–169896, 2020.

[37] R. C. Gonzalez and R. E. Woods, *Digital Image Processing*. Upper Saddle River, NJ, USA: Prentice-Hall, 2008.

[38] Y.-T. Kim, "Quantized bi-histogram equalization," in *Proc. IEEE Int. Conf. Acoust., Speech, Signal Process.*, Munich, Germany, Apr. 1997, pp. 2797–2800.

[39] Y.-T. Kim, "Contrast enhancement using brightness preserving bi-histogram equalization," *IEEE Trans. Consum. Electron.*, vol. 43, no. 1, pp. 1–8, Feb. 1997.

[40] V. Stimper, S. Bauer, R. Ernstorfer, B. Scholkopf, and R. P. Xian, "Multidimensional contrast limited adaptive histogram equalization," *IEEE Access*, vol. 7, pp. 165437–165447, 2019.
[41] D. Menotti, L. Najman, J. Facon, and A. A. Araujo, "Multi-histogram equalization methods for contrast enhancement and brightness preserving," *IEEE Trans. Consum. Electron.*, vol. 53, no. 3, pp. 1186–1194, Aug. 2007.
[42] A. Mehrish, A. V. Subramanyam, and S. Emmanuel, "Joint spatial and discrete cosine transform domain-based counter forensics for adaptive contrast enhancement," *IEEE Access*, vol. 7, pp. 27183–27195, 2019.
[43] C. Ding, X. Pan, X. Gao, L. Ning, and Z. Wu, "Three adaptive sub-histograms equalization algorithm for maritime image enhancement," *IEEE Access*, vol. 8, pp. 147983–147994, 2020.
[44] S. M. Pizer, E. P. Amburn, J. D. Austin, R. Cromartie, A. Geselowitz, T. Greer, B. ter Haar Romeny, J. B. Zimmerman, and K. Zuiderveld, "Adaptive histogram equalization and its variations," *Comput. Vis., Graph., Image Process.*, vol. 39, no. 3, pp. 355–368, 1987.
[45] J.-Y. Kim, L.-S. Kim, and S.-H. Hwang, "An advanced contrast enhancement using partially overlapped sub-block histogram equalization," *IEEE Trans. Circuits Syst. Video Technol.*, vol. 11, no. 4, pp. 475–484, Apr. 2001.
[46] W. Wang, X. Wu, X. Yuan, and Z. Gao, "An experiment-based review of low-light image enhancement methods," *IEEE Access*, vol. 8, pp. 87884–87917, 2020.
[47] K. Zuiderveld, "Contrast limited adaptive histogram equalization," in *Proc. Graph. Gems*, 1994, pp. 474–485.
[48] Y. Chang, C. Jung, P. Ke, H. Song, and J. Hwang, "Automatic contrast-limited adaptive histogram equalization with dual gamma correction," *IEEE Access*, vol. 6, pp. 11782–11792, Mar. 2018.
[49] NASA. (2001). *Retinex Image Processing*. [Online]. Available: http://dragon.larc.nasa.gov/retinex/
[50] S. W. Hasinoff, D. Sharlet, R. Geiss, A. Adams, J. T. Barron, F. Kainz, J. Chen, and M. Levoy, "Burst photography for high dynamic range and low-light imaging on mobile cameras," *ACM Trans. Graph.*, vol. 35, no. 6, pp. 1–12, Nov. 2016.
[51] T. Celik and T. Tjahjadi, "Contextual and variational contrast enhancement," *IEEE Trans. Image Process.*, vol. 20, no. 12, pp. 3431–3441, Dec. 2011.
[52] C. Lee, C. Lee, and C.-S. Kim, "Contrast enhancement based on layered difference representation of 2D histograms," *IEEE Trans. Image Process.*, vol. 22, no. 12, pp. 5372–5384, Dec. 2013.
[53] T. Arici, S. Dikbas, and Y. Altunbasak, "A histogram modification framework and its application for image contrast enhancement," *IEEE Trans. Image Process.*, vol. 18, no. 9, pp. 1921–1935, Sep. 2009.
[54] X. Fu, D. Zeng, Y. Huang, X.-P. Zhang, and X. Ding, "A weighted variational model for simultaneous reflectance and illumination estimation," in *Proc. IEEE Conf. Comput. Vis. Pattern Recognit. (CVPR)*, Las Vegas, NV, USA, Jun. 2016, pp. 2782–2790.
[55] A. Mittal, A. K. Moorthy, and A. C. Bovik, "No-reference image quality assessment in the spatial domain," *IEEE Trans. Image Process.*, vol. 21, no. 12, pp. 4695–4708, Dec. 2012.
[56] L. Zhang, L. Zhang, X. Mou, and D. Zhang, "FSIM: A feature similarity index for image quality assessment," *IEEE Trans. Image Process.*, vol. 20, no. 8, pp. 2378–2386, Aug. 2011.
[57] S. S. Agaian, K. Panetta, and A. M. Grigoryan, "Transform-based image enhancement algorithms with performance measure," *IEEE Trans. Image Process.*, vol. 10, no. 3, pp. 367–382, Mar. 2001.
[58] K. Gu, D. Tao, J.-F. Qiao, and W. Lin, "Learning a no-reference quality assessment model of enhanced images with big data," *IEEE Trans. Neural Netw. Learn. Syst.*, vol. 29, no. 4, pp. 1301–1313, Apr. 2018.
[59] A. Mittal, R. Soundararajan, and A. C. Bovik, "Making a 'completely blind' image quality analyzer," *IEEE Signal Process Lett.*, vol. 20, no. 3, pp. 209–212, Mar. 2013.

**TZU-CHIA TUNG** received the B.S. degree in computer science and information engineering from Chung Hua University, in 2012, and the M.S. degree in computer science and information engineering from National Dong Hwa University, in 2016. He is currently pursuing the Ph.D. degree with the Graduate Institute of Networking and Multimedia, National Taiwan University. His research interests include computer vision, image processing, pattern recognition, and machine learning.

**CHIOU-SHANN FUH** (Member, IEEE) received the B.S. degree in computer science and information engineering from National Taiwan University, Taipei, in 1983, the M.S. degree in computer science from Pennsylvania State University, University Park, in 1987, and the Ph.D. degree in computer science from Harvard University, Cambridge, MA, USA, in 1992. From 1992 to 1993, he was with AT&T Bell Laboratories, where he was engaged in performance monitoring of switching networks. From 1993 to 2000, he was an Associate Professor with the Department of Computer Science and Information Engineering, National Taiwan University, Taipei, where he was promoted to a Full Professor. His current research interests include digital image processing, computer vision, pattern recognition, mathematical morphology, and their applications to defect inspection, industrial automation, digital still camera, digital video camcorder, and camera module such as color interpolation, auto exposure, auto focus, auto white balance, color calibration, and color management.